

# NISQ Algorithm for Semidefinite Programming

Kishor Bharti,<sup>1,\*</sup> Tobias Haug,<sup>2</sup> Vlatko Vedral,<sup>1,3</sup> and Leong-Chuan Kwek<sup>1,4,5,6</sup>

<sup>1</sup>*Centre for Quantum Technologies, National University of Singapore, 3 Science Drive 2, Singapore 117543*

<sup>2</sup>*QOLS, Blackett Laboratory, Imperial College London SW7 2AZ, UK*

<sup>3</sup>*Clarendon Laboratory, University of Oxford, Parks Road, Oxford OX1 3PU, United Kingdom*

<sup>4</sup>*MajuLab, CNRS-UNS-NUS-NTU International Joint Research Unit, UMI 3654, Singapore*

<sup>5</sup>*National Institute of Education, Nanyang Technological University, 1 Nanyang Walk, Singapore 637616*

<sup>6</sup>*School of Electrical and Electronic Engineering Block S2.1, 50 Nanyang Avenue, Singapore 639798*

Semidefinite Programming (SDP) is a class of convex optimization programs with vast applications in control theory, quantum information, combinatorial optimization and operational research. Noisy intermediate-scale quantum (NISQ) algorithms aim to make an efficient use of the current generation of quantum hardware. However, optimizing variational quantum algorithms is a challenge as it is an NP-hard problem that in general requires an exponential time to solve and can contain many far from optimal local minima. Here, we present a current term NISQ algorithm for SDP. The classical optimization program of our NISQ solver is another SDP over a smaller dimensional ansatz space. We harness the SDP based formulation of the Hamiltonian ground state problem to design a NISQ eigensolver. Unlike variational quantum eigensolvers, the classical optimization program of our eigensolver is convex, can be solved in polynomial time with the number of ansatz parameters and every local minimum is a global minimum. Further, we demonstrate the potential of our NISQ SDP solver by finding the largest eigenvalue of up to  $2^{1000}$  dimensional matrices and solving graph problems related to quantum contextuality. We also discuss NISQ algorithms for rank-constrained SDPs. Our work extends the application of NISQ computers onto one of the most successful algorithmic frameworks of the past few decades.

The panorama of quantum computing has been transformed enormously in the last forty years. Once acknowledged as a theoretical pursuit, quantum computers with a few dozen qubits are now a reality. Advancement at the hardware frontier has led to the demonstration of “computational quantum supremacy” for contrived tasks [1, 2]. We sit at the edge of the noisy intermediate-scale quantum (NISQ) era [3, 4]. In recent years, significant effort has been put towards designing algorithms for practically relevant tasks which can be implemented on NISQ devices [4, 5]. Canonical examples of these NISQ algorithms are variational quantum algorithms (VQAs) such as the variational quantum eigensolver (VQE) [6–8] and the quantum approximate optimization algorithm (QAOA) [9, 10]. NISQ algorithms have been developed for various tasks such as finding the ground state of Hamiltonians [6–8, 11–22], combinatorial optimization [9, 10], quantum simulation [23–36] quantum metrology [37, 38] and machine learning [39–43]. These algorithms have been investigated in detail with a comprehensive exposition on possible hurdles [44–49] and corresponding countermeasures [49–52]. A thorough study of possible applications of NISQ devices is expected to unravel the potential as well as limitations of such devices. Moreover, in the quest for practical quantum advantage in the NISQ era it is pertinent to investigate novel NISQ algorithms for practically relevant tasks.

A major challenge in the NISQ era is the optimization program for VQAs, where a classical optimizer is

searching for the parameters of a quantum state that minimizes a cost function. For the VQA to be successful, one requires an ansatz that is expressible enough to approximate the optimal solution of the corresponding optimization problem. However, even if such ansatz has been found, the optimization program of the VQA is NP-hard and the optimization landscape contains numerous far from optimal persistent local minima [48]. The highly non-convex nature of landscape renders optimization difficult even for VQAs involving logarithmically many qubits or classically easy problems such as free fermions.

In the last few decades, semidefinite programming (SDP) has led to ground breaking developments in mathematical optimization [53, 54]. The study of SDP has uncovered numerous applications in theoretical computer science, control theory and operations research. Many problems in quantum information such as state discrimination [55, 56], dimension witness [57] and self-testing [58–60] can be investigated using SDPs. While SDPs can be solved efficiently in polynomial time on classical computers, high dimensional problems may still be out of scope for classical computers. For example, finding the ground state of a Hamiltonian can be framed as an SDP, however it is intractable for classical computers due to the exponential scaling of the dimension of the problem. To explore possible quantum advantages for solving SDPs with quantum computers, quantum SDP solvers have been studied comprehensively [61–65]. However, existing quantum SDP solvers cannot be executed on NISQ devices as they require extensive quantum resources.

Here, we propose the NISQ SDP Solver (NSS) as a hybrid quantum-classical algorithm to solve SDPs. The

---

\* kishor.bharti1@gmail.com

NSS encodes a SDP onto a quantum computer combined with an optimization routine on a classical computer. The classical optimization part of the NSS is also an SDP with its dimension given by the size of the ansatz space. The quantum computational part of the NSS has no classical-quantum feedback loop and requires the quantum computer only for estimating overlaps, which can be done efficiently on current NISQ devices. We showcase the NSS for a wide range of problems. We design a NISQ SDP based quantum eigensolver (NSE) to find the ground state of quantum Hamiltonians. In contrast to VQE, the classical optimization part of the NSE can be solved in polynomial time without the local minima problem. The NSS can be employed for finding the largest eigenvalue of matrices, which we demonstrate for matrices as large as  $2^{1000}$ . Finally, we show the NSS for various important problems related to quantum information such as Bell non-local games and the Lovász Theta number. We also provide the extension of the NSS for rank-constrained SDPs.

We now highlight the key difference between VQA and NSS in Fig.1 by using the ground state problem as an example. Finding the ground state of a Hamiltonian can be framed as an SDP using density matrices (see program 10), however the SDP suffers from exponential scaling of the dimension of the quantum state and thus it is difficult to solve on classical computers. To address the scaling of the quantum state, VQE and NSE map the quantum state onto a quantum computer. VQE uses a quantum circuit parameterized by the parameter  $\theta$ . Then, the VQE minimizes the energy of the quantum state by variationally adjusting the parameter  $\theta$  via a classical optimization routine in a feedback loop. However, this minimization task is challenging as the corresponding optimization program is NP-hard. In particular, the energy as function of  $\theta$  is non-convex with persistent far from optimal local minima [48], where optimization routines struggle to find the global minima. In contrast, the NSE uses a hybrid density matrix (4). It consists of a linear combination of a  $M$ -dimensional set of ansatz quantum states with classical combination coefficients  $\beta$ . In the NSS, the  $\beta$  parameters are optimised to minimize the energy. The optimization of the coefficients  $\beta$  is another SDP with dimension  $M$  only, which can be efficiently optimised in polynomial time on a classical computer. The ansatz preserves the convexity of the landscape and hence any local minimum is also a global minimum.

## I. SEMIDEFINITE PROGRAMMING

SDP can be thought of as generalization of the “standard form” linear programming (LP). The

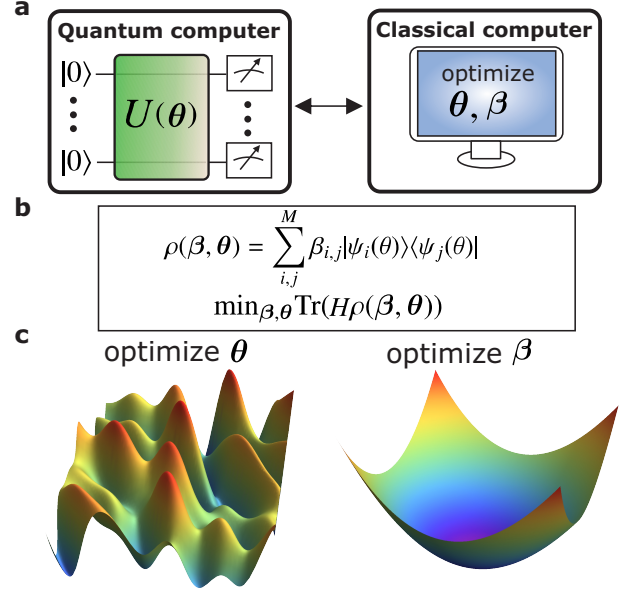


FIG. 1. **a)** Hybrid quantum-classical computing approach to NISQ. Quantum computer prepares and measures  $M$  quantum states  $|\psi_i(\theta)\rangle$ . Classical computer is used to optimize hybrid density matrix  $\rho(\beta, \theta) = \sum_{i,j}^M \beta_{i,j} |\psi_i(\theta)\rangle\langle\psi_j(\theta)|$ , which depends on the parameters for the parameterized quantum circuit  $\theta$  and the combination coefficients  $\beta$ . **b)** Optimization task to find ground state of Hamiltonian  $H$  by minimizing parameters  $\beta, \theta$  in respect to energy  $\text{Tr}(H\rho(\beta, \theta))$ . **c)** Landscape of optimization task for  $\beta$  and  $\theta$ . Optimization of  $\theta$  in the variational quantum eigensolver (VQE) is NP-hard with a non-convex landscape and persistent far from optimal local minima. Optimisation of  $\beta$  in the NISQ SDP based eigensolver (NSE) can be solved in polynomial time by a semidefinite program (SDP), where the optimisation landscape is convex. Due to the convexity of the optimisation landscape, any local minimum is also a global minimum.

“standard form” of LP is given by

$$\begin{aligned} \min \quad & c^T x \\ \text{s.t.} \quad & a_i^T x = b_i \quad \forall i \in [m] \\ & x \in \mathbb{R}_+^n, \end{aligned} \tag{1}$$

where the set  $[m]$  is given by  $[m] \equiv \{1, 2, 3, \dots, m\}$ . Here,  $\mathbb{R}_+^n := \{x \in \mathbb{R}^n | x \geq 0\}$ . The set  $\mathbb{R}_+^n$  is known as nonnegative orthant. The phrase “standard form” hints that there are other possible non-standard representations of LPs. Any LP in non-standard form, however, can be converted into standard form by following a few tricks. These tricks include change of variables, transforming the inequalities into equalities and switching maximum to minimum.

In SDP, the non-negativity constraint  $x \geq 0$  is replaced by positive semidefinite cone constraint  $X \succcurlyeq 0$ . SDP involves optimization of a linear function of matrix  $X$  over the affine slice of the cone of positive semidefinite

matrices. The standard form of an SDP is given by

$$\begin{aligned} \min & \text{Tr}(CX) \\ \text{s.t.} & \text{Tr}(A_i X) = b_i \quad \forall i \in [m] \\ & X \in \mathcal{S}_+^n. \end{aligned} \quad (2)$$

Here,  $\mathcal{S}_+^n$  denotes the set of  $n \times n$  symmetric positive semidefinite matrices. Mathematically speaking,  $\mathcal{S}_+^n := \{X \in \mathcal{S}^n | X \succcurlyeq 0\}$ . The matrices  $C$  and  $A_i$  belong to the set of symmetric matrices  $\mathcal{S}^n$  for  $i \in [m]$ . The  $i$ -th element of vector  $b \in \mathbb{R}^m$  is denoted by  $b_i$ .

Duality is one of the oldest and most fruitful ideas in mathematics. The duality principle of mathematical optimization theory suggests that mathematical optimization problems can be viewed from either of two perspectives, namely the primal problem or the dual problem. For a given primal minimization problem  $P$ , the solution to the corresponding dual problem  $D$  provides a lower bound to the solution of  $P$ . The standard form of the dual of the SDP in program 2 is given by

$$\begin{aligned} \max & b^T y \\ \text{s.t.} & \sum_{i=1}^m y_i A_i \preccurlyeq C \\ & y \in \mathbb{R}^m. \end{aligned} \quad (3)$$

The SDPs in programs 2 and 3 constitute a primal-dual pair. SDP can be extended to complex-valued matrices via a cone of Hermitian positive semidefinite matrices i.e.  $X \in \mathcal{H}_+^n$ . Here,  $\mathcal{H}_+^n$  denotes the set of  $n \times n$  Hermitian positive semidefinite matrices. Since SDP for complex-valued matrices is more general than SDP for real valued matrices, we will consider the former case in this work.

## II. THE NSS

We now outline the NSS, which consists of three distinct steps, namely ansatz selection, overlap measurement and post-processing. First, we select a set of quantum states  $\mathbb{S} = \{|\psi_j\rangle \in \mathcal{H}\}_j$  over a Hilbert space  $\mathcal{H}$ , where the set contains  $M$  quantum states  $|\mathbb{S}| = M$ . Now, our NISQ semidefinite programming solver (NSS) uses the following hybrid density matrix ansatz

$$X_\beta = \sum_{(|\psi_i\rangle, |\psi_j\rangle) \in \mathbb{S} \times \mathbb{S}} \beta_{i,j} |\psi_i\rangle \langle \psi_j|, \quad (4)$$

where  $\beta_{i,j} \in \mathbb{C}$ . Note that the quantum states in  $\mathbb{S}$  are prepared by a quantum system while the coefficients  $\beta_{i,j}$  are stored on some classical device as matrix  $\beta$ . For  $\beta \in \mathcal{H}_+^M$ , we have  $X_\beta \in \mathcal{H}_+^n$  (see Appendix B). We now assume that  $C$  and constraint matrices  $A_i$  of program 2

can be written as a sum of unitaries

$$\begin{aligned} C &= \sum_k s_k U_k \\ A_i &= \sum_l f_{i,l} U_l^{(i)}. \end{aligned}$$

As second step of the NSS, we measure the following overlaps on the quantum system

$$\mathcal{D}_{a,b} = \sum_k s_k \langle \psi_b | U_k | \psi_a \rangle \quad (5)$$

$$\mathcal{E}_{a,b}^{(i)} = \sum_l f_{i,l} \langle \psi_b | U_l^{(i)} | \psi_a \rangle. \quad (6)$$

The overlaps can be measured using the Hadamard test or with direct measurement methods [66]. An alternative NISQ-friendly method that requires only sampling in the computational basis has been proposed in [21]. This method assumes that the unitaries  $U_k$  and  $U_l^{(i)}$  are Pauli strings  $P = \bigotimes_{j=1}^N \sigma_j$  with  $\sigma \in \{I, \sigma^x, \sigma^y, \sigma^z\}$ . As the Pauli strings form a complete basis, any matrix can be decomposed into a linear combination of Pauli strings. Further, we assume that the ansatz space is generated by a state  $|\psi\rangle$  and a set of  $M$  different Pauli strings  $\{P_1, \dots, P_M\}$  via  $\mathbb{S} = \{P_j |\psi\rangle\}_{j=1}^M$ . Now, each overlap element in (5), (6) can be written as a sum of expectation values of Pauli strings  $\langle \psi | P_1 P_2 P_3 | \psi \rangle = a \langle \psi | P' | \psi \rangle$ , where we use that a product of Pauli strings can be written as a single Pauli string  $P'$  with a prefactor  $a \in \{+1, -1, +i, -i\}$ . Then, one can efficiently calculate the overlap elements by measuring the expectation values of Pauli strings. On NISQ computers, this can be done by single-qubit rotations into the eigenbasis of the Pauli operator and sampling in the computational basis. We emphasize that for the choice of quantum states of the form  $\mathbb{S} = \{P_j |\psi\rangle\}_{j=1}^M$ , one only needs to prepare the reference state  $|\psi\rangle$ . Other states are related to the reference state via single layer Pauli unitaries. In such cases, the second step of our algorithm requires sampling  $|\psi\rangle$  in a set of Pauli rotated basis elements.

The third and final step of the NSS consists of post-processing on a classical computer. Here, we write the standard form primal SDP in terms of the measured overlaps

$$\begin{aligned} \min & \text{Tr}(\beta \mathcal{D}) \\ \text{s.t.} & \text{Tr}(\beta \mathcal{E}^{(i)}) = b_i \quad \forall i \in [m] \\ & \beta \in \mathcal{H}_+^M. \end{aligned} \quad (7)$$

This is an SDP over  $\beta$  with the corresponding hybrid density matrix is given by (4). The dual of the SDP in program 7 is given by

$$\begin{aligned} \max & b^T y \\ \text{s.t.} & \sum_{i=1}^m y_i \mathcal{E}^{(i)} \preccurlyeq \mathcal{D}. \end{aligned} \quad (8)$$

The SDPs in program 7 and 8 constitute a primal-dual pair over the ansatz space that can be solved in polynomial time on a classical computer. In the case where the ansatz states  $|\psi_i\rangle$  are linear independent and cover the whole Hilbert space, the programs 7 and 8 over the ansatz space recover the SDPs over entire space corresponding to programs 2 and 3.

### III. EXTENSIONS TO RANK-CONSTRAINED SDPS

Rank constrained SDPs find numerous applications in combinatorics [67], control theory [68] and quantum information [57]. Many problems in optimization theory can be modelled as rank-constrained SDPs [53, 69]. The presence of the rank-constraint renders the optimization program to be non-convex. Solving rank-constrained SDPs is NP-hard and hence they are computationally intractable. The optimization program for rank constrained SDPs is given by

$$\begin{aligned} \min \quad & \text{Tr}(CX) \\ \text{s.t.} \quad & \text{Tr}(A_i X) = b_i \quad \forall i \in [m] \\ & \text{rank}(X) \leq k \\ & X \in \mathcal{S}_+^n. \end{aligned} \quad (9)$$

Notice that the only difference between the regular SDP in program 2 and the rank-constrained SDP in program 9 is the presence of the rank constraint  $\text{rank}(X) \leq k$  in the latter. Intuitively speaking, the aforementioned rank constraint means that the optimizer of the program 9 must have a rank of at most  $k$ . The famous Max-Cut problem can be modelled as a rank constrained SDP for  $k = 1$  (see Appendix C). We defer the extension of the NSS for the rank constrained SDPs in Appendix C.

### IV. EXAMPLES

We now demonstrate the NSS for various problems of interest.

#### A. Ground State Problem

One of the special cases of NSS is the NISQ SDP based eigensolver (NSE). For Hamiltonian  $H$  and density matrix  $\rho$ , the problem of finding the ground state can be written as

$$\begin{aligned} \min \quad & \text{Tr}(\rho H) \\ \text{s.t.} \quad & \text{Tr}(\rho) = 1 \\ & \rho \succeq 0. \end{aligned} \quad (10)$$

The dual formulation for the program in 10 is given by

$$\begin{aligned} \max \quad & \lambda \\ \text{s.t.} \quad & (H - \lambda I) \succeq 0. \end{aligned} \quad (11)$$

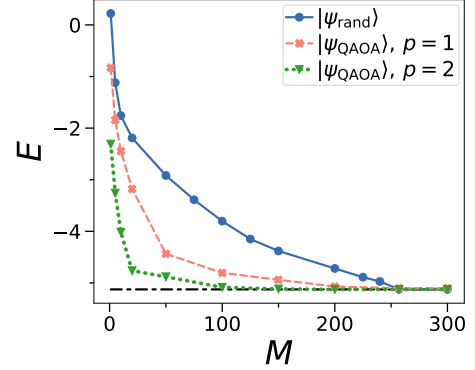


FIG. 2. Ground state energy  $E$  of the transverse Ising model ( $h = 1$ ) calculated via NSE plotted against number of ansatz states  $M$ . Ansatz states are generated by applying  $M$  Pauli strings on a randomized hardware efficient circuit composed of  $p = 4$  layers of single qubit  $y$  rotations and CNOT gates arranged in a chain topology (solid blue line) or a optimized QAOA ansatz with number of layers  $p = 1$  (dashed orange line) and  $p = 2$  (dotted green line). Black dashed-dotted line is the exact ground state energy for  $N = 8$  qubits.

The optimum value of  $\lambda$  corresponds to the ground state energy. In the ansatz space generated by  $\mathcal{S}$ , the primal SDP for the Hamiltonian ground state problem is given by

$$\begin{aligned} \min \quad & \text{Tr}(\beta \mathcal{D}) \\ \text{s.t.} \quad & \text{Tr}(\beta \mathcal{E}) = 1 \\ & \beta \in \mathcal{H}_+^M. \end{aligned} \quad (12)$$

The dual program for 12 is given by

$$\begin{aligned} \max \quad & \lambda \\ \text{s.t.} \quad & (\mathcal{D} - \lambda \mathcal{E}) \succeq 0. \end{aligned} \quad (13)$$

Notice that the primal optimization program over  $\beta$  is convex and hence exhibits a unique minimum value. This is unlike the case of VQE, where optimization is non-convex and there can be multiple local minima [48]. In the NSE, the classical optimization finds the optimal solution in time polynomial in the number of ansatz parameters, given that the solution is contained in the ansatz space. On the other hand, in VQAs such as VQE and QAOA, even if the optimal solution is contained in the ansatz space, the classical optimization can be NP-hard [48].

In Fig.2, we demonstrate the NSE for finding the ground state for the transverse Ising model  $H_{\text{ising}} = \sum_{n=1}^N \sigma_n^z \sigma_{n+1}^z + h \sigma_n^x$  with  $N$  qubits. We construct the ansatz space using a quantum state  $|\psi\rangle$ . We choose a hardware efficient ansatz  $|\psi_{\text{rand}}\rangle$  consisting  $p$  layers of randomized  $y$ -rotations and CNOT gates arranged in a chain topology (see Appendix A) and the QAOA ansatz  $|\psi_{\text{QAOA}}(\gamma, \delta)\rangle = \prod_{k=1}^p e^{-i\delta_k \sum_{n=1}^N \sigma_n^x} e^{-i\gamma_k \sum_{n=1}^N \sigma_n^z \sigma_{n+1}^z} |+\rangle$  with depth  $p$  [9], where we have optimized the  $\gamma$  and



$\delta$  parameters beforehand. The  $M$ -dimensional ansatz space  $\mathbb{S}$  is generated via the  $K$ -moment expansion [21]. The cumulative  $K$ -moment states are generated by applying Pauli operators on the quantum state  $|\psi\rangle$ . This yields the set  $\mathbb{CS}_K = \{|\psi\rangle\} \cup \{P_{i_1}|\psi\rangle\}_{i_1=1}^r \cup \dots \cup \{U_{i_K} \dots P_{i_1}|\psi\rangle\}_{i_1=1, \dots, i_K=1}^r$ , where  $P_i$  are the  $r$  Pauli strings that make up  $H_{\text{ising}} = \sum_{i=1}^r s_i P_i$ . We pick the first  $M$  elements from the cumulative  $K$ -moment states to get the ansatz space  $\mathbb{S}$ . We find that with increasing  $M$  the energy converges to the ground state, where the QAOA ansatz converges already for a lower number of  $M$ .

### B. Largest Eigenvalue

Our next task is to find the largest eigenvalue of a sparse matrix  $C$  by maximizing program 12. We assume that  $C$  is of size  $\mathcal{N} = 2^N$  and is represented by a combination of  $S$  Pauli string  $C = \sum_{i=1}^S c_i P_i^r$ , where the Pauli strings are given by  $P_i^r = \otimes_{j=1}^N \sigma_j$  with  $\sigma_j \in \{I, \sigma^x, \sigma^y, \sigma^z\}$  and  $c_i$  is a prefactor. To numerically demonstrate the performance of NSS, we uniformly sample the Pauli operators for each qubit, choose random  $c_i \in [-1, 1]$  and use the  $N$ -bit state with all zeros  $|0\rangle^{\otimes N}$  as ansatz state. Using the idea of cumulative  $K$ -moment states, we construct the ansatz space  $\mathbb{S}$  using products of  $P_i^r$ . While the expectation values can be calculated classically for the product state, it becomes intractable for general quantum states. In Fig. 3, we plot the difference between the largest eigenvalue found by NSE and the exact solution  $\Delta\lambda$  as function of the number of states  $M$  within the ansatz space for different matrix dimensions  $\mathcal{N}$ . We find good convergence even for matrix dimensions  $2^{1000}$ .

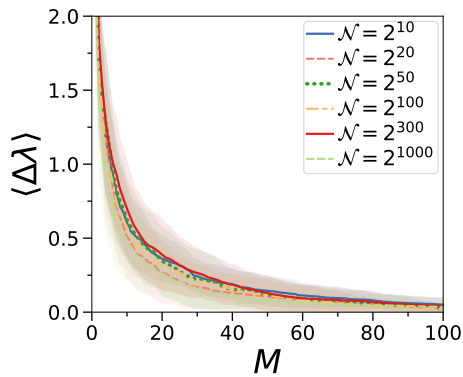


FIG. 3. NSS for calculating the largest eigenvalue of a matrix  $C$  consisting of  $S = 8$  random Pauli strings. We show average difference  $\langle \Delta\lambda \rangle$  between largest eigenvalue found by NSE and exact largest eigenvalue as function of ansatz space  $M$  for different matrix sizes  $\mathcal{N}$ . Shaded area is standard deviation of  $\Delta\lambda$  averaged over 20 random instances of  $C$ .

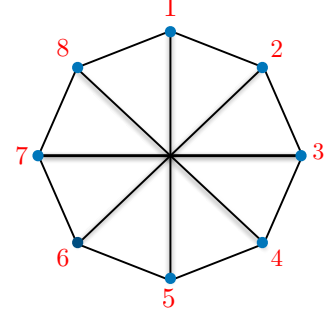


FIG. 4. Graph with 8 nodes that has applications in quantum foundations and in device certification protocols. We calculate the Lovász Theta number  $(2 + \sqrt{2})$  for this graph using NSS.

### C. Lovász Theta Number

Graph invariants are properties that depend only on the abstract structure of a graph. The Lovász Theta number is such a graph invariant that was first introduced by László Lovász in the breakthrough 1979 paper titled “On the Shannon capacity of a Graph” [70]. The Lovász Theta number provides an upper bound to the Shannon capacity of a graph, another graph invariant quantity. Surprisingly, it is connected with quantum contextuality [58–60, 71–73] and can help us to understand the potential of quantum computers [74]. Given a graph  $G = (V, E)$  with vertex set  $V$  and adjacency matrix  $E$ , the SDP for the Lovász Theta number is given by

$$\begin{aligned} \max \quad & \text{Tr}(JX) \\ \text{s.t.} \quad & X_{i,j} = 0 \quad \forall E_{i,j} = 1 \\ & \text{Tr}(X) = 1 \\ & X \succeq 0. \end{aligned} \tag{14}$$

Here,  $J$  is an all one matrix. Since  $X$  is real valued, the ansatz space can be taken as real valued, which can be achieved within NSS by demanding that the ansatz quantum states are real valued. To demonstrate the NSS, we calculate the Lovász Theta number for the graph shown in Fig. 4. To generate the ansatz states  $\mathbb{S}$ , we apply a set of Pauli operators on a quantum state. We use the zero state  $|0\rangle = |0\rangle^{\otimes N}$  or representative examples of randomized states generated via hardware efficient quantum circuits  $|\psi_{\text{rand}}\rangle$  (see Appendix A). Then, the set of basis states is generated by applying  $M$  different combinations of Pauli strings on the state  $\mathbb{S} = \{P_i^x |\psi\rangle\}_{i=1}^M$ , where  $P_i^x = \otimes_{j=1}^N \sigma_j$  with  $\sigma_j \in \{I, \sigma^x\}$ . In Fig. 5a we show the error of the NSS. We calculate the error as the difference between the exact solution  $C_{\text{exact}}$ , including the constraints of the problem, and the expectation values  $\langle C \rangle$  gained from the quantum state via NSS. We observe an improvement with increasing number of ansatz states  $M$ , reaching the optimal solution

latest when the number of basis states reaches the dimension of the problem. Depending on the choice of basis states, the optimal solution can be reached with a lower number of ansatz states.

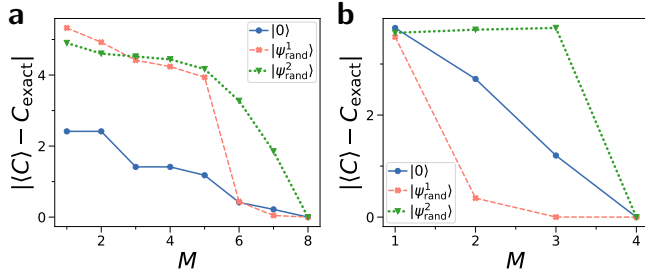


FIG. 5. Error of exact solution  $C_{\text{exact}}$  and NSS  $\langle C \rangle$  plotted against number of ansatz states  $M$ .  $C_{\text{exact}}$  and  $\langle C \rangle$  are vectors that contain the cost function as well as the constraints to be fulfilled. The ansatz space is generated using the all zero state  $|0\rangle$  as well as representative examples of randomized quantum circuit  $|\psi_{\text{rand}}\rangle$  constructed in a hardware efficient manner using  $p = 4$  layers of single qubit  $y$  rotations and CNOT gates arranged in a chain topology. With these states, we generate the  $M$  basis states  $\mathbb{S} = \{P_i^x |\psi\rangle\}_{i=1}^M$ , where  $P_i^x$  is one of the  $N$ -qubit Pauli strings consisting of identity  $I$  and  $\sigma^x$  operators. **a)** NSS algorithm for Lovász Theta number for the graph given in Fig.4 with  $N = 3$  qubits. **b)** Bell non-local game with  $N = 2$  qubits.

#### D. Bell Non-Locality

Finally we apply the NSS to calculate the quantumly achievable success probability for the canonical Bell non-local game: the Clauser Horn Shimony Holt (CHSH) game [75–78]. The CHSH game involves two spacelike separated parties, say Alice and Bob. A referee asks the players uniformly random pairs of questions  $x, y \in \{0, 1\}$ . The players have to answer  $a, b \in \{0, 1\}$  such that

$$a \oplus b = x \wedge y. \quad (15)$$

Here  $\oplus$  denotes addition modulo 2 and  $\wedge$  is the logical AND operator. Using classical strategies, the maximum probability of success for the CHSH game is upper bounded by 0.75. However, using quantum resources such as entangled states, the players can win the game with probability  $\cos^2(\frac{\pi}{8})$ . The success probability for the CHSH game can be calculated using SDP. For details, see Appendix D. We implemented the aforementioned SDP using NSS in Fig.5b using the same ansatz as for the Lovász Theta number and find that for sufficient number of basis states  $M$  we achieve the correct result.

#### V. CONCLUSION

We presented the NSS for solving SDPs, including rank-constrained SDPs. Our algorithm runs on NISQ

devices without the need for classical-quantum feedback loops, requiring only the measurement of overlaps on the quantum computer. If the input matrices of the SDP ( $C$  and  $A_i$ s) are linear combinations of Pauli strings, the aforementioned overlaps can be obtained by sampling the reference state  $|\psi\rangle$  in a Pauli rotated basis.

The ground state problem expressed in terms of density matrices is a SDP and hence a convex optimization program. However, the SDP corresponding to the ground state problem suffers from exponential scaling of the dimension of the quantum state, rendering it difficult to solve on classical computers. To tackle the exponential scaling of the dimension, VQEs employ optimization over smaller dimensional ansatz space. As shown recently, the classical optimization corresponding to VQEs is NP-hard, and the landscape contains numerous far from optimal persistent local minima [48]. We employed our NSS to develop the NSE, a NISQ algorithm for the ground state problem. The key idea of our NSE is to optimize over a smaller number of parameters while preserving the convexity of the original problem. Unlike VQEs, our optimization program is convex, and thus every local minimum is a global minimum. Moreover, the classical optimization program of the NSE is a SDP that can be solved in polynomial-time.

The previously proposed quantum assisted eigensolver and iterative quantum assisted eigensolvers [20, 21] are special cases of our rank constrained SDP solver with unit rank (see Appendix C). With our NSS, it is now possible to solve various important problems that can be formulated in terms of SDPs in a NISQ setting. Our work unlocks the possibility of running one of the most important algorithmic frameworks of classical computing on NISQ computers and exploring the capabilities of the current generation quantum computers. We implemented the NSS to calculate Lovász Theta number, a graph invariant with various applications, including in quantum contextuality. Further, we used our algorithm to determine the maximum winning probability of Bell nonlocal games. We demonstrated the applicability of our algorithm for finding the largest eigenvalue of matrices of a size as large as  $2^{1000}$ .

Our work leads to many novel avenues for future research. Investigating a systematic problem aware strategy for determining the reference state  $|\psi\rangle$  and the basis states  $|\psi_i\rangle$  used to construct the hybrid density matrix will help improve as well as understand the NSS and its rank constrained variants. It would be fascinating to study our algorithms in the presence of noise. Further, analysing our algorithms to render complexity-theoretic statements is another exciting direction for further investigation.

The ground state problem can be thought of as quantum native problem in the sense that the exponential scaling of the Hilbert space size makes it challenging to solve with classical devices. This problem can be framed as a convex optimization program over density matrices. Thus, we could conceive the ground state problem as a

“convex quantum native problem”. In future, it would be interesting to employ techniques from our work to other convex quantum native problems from disciplines such as quantum chemistry, condensed matter physics and quantum information.

The Quantum interior-point method [64] and quantum multiplicative weight approaches [61–63] have been proposed in the literature to solve SDPs. It would be interesting to develop the corresponding NISQ algorithms. Extending our work to the general case of cone programming seems another exciting direction.

Python code for the numerical calculations performed are available at [79].

*Acknowledgements*— We thank Atul Singh Arora for interesting discussions. We are grateful to the National Research Foundation and the Ministry of Education, Singapore for financial support. This work is supported by a Samsung GRC project and the UK Hub in Quantum Computing and Simulation, part of the UK National Quantum Technologies Programme with funding from UKRI EPSRC grant EP/T001062/1.

- 
- [1] F. Arute, K. Arya, R. Babbush, D. Bacon, J. C. Bardin, R. Barends, R. Biswas, S. Boixo, F. G. Brandao, D. A. Buell, *et al.*, *Nature* **574**, 505 (2019).
  - [2] H.-S. Zhong, H. Wang, Y.-H. Deng, M.-C. Chen, L.-C. Peng, Y.-H. Luo, J. Qin, D. Wu, X. Ding, Y. Hu, *et al.*, *Science* **370**, 1460 (2020).
  - [3] J. Preskill, *Quantum* **2**, 79 (2018).
  - [4] K. Bharti, A. Cervera-Lierta, T. H. Kyaw, T. Haug, S. Alperin-Lea, A. Anand, M. Degroote, H. Heimonen, J. S. Kottmann, T. Menke, *et al.*, arXiv preprint arXiv:2101.08448 (2021).
  - [5] M. Cerezo, A. Arrasmith, R. Babbush, S. C. Benjamin, S. Endo, K. Fujii, J. R. McClean, K. Mitarai, X. Yuan, L. Cincio, *et al.*, arXiv preprint arXiv:2012.09265 (2020).
  - [6] A. Peruzzo, J. McClean, P. Shadbolt, M.-H. Yung, X.-Q. Zhou, P. J. Love, A. Aspuru-Guzik, and J. L. O’Brien, *Nature communications* **5**, 4213 (2014).
  - [7] J. R. McClean, J. Romero, R. Babbush, and A. Aspuru-Guzik, *New Journal of Physics* **18**, 023023 (2016).
  - [8] A. Kandala, A. Mezzacapo, K. Temme, M. Takita, M. Brink, J. M. Chow, and J. M. Gambetta, *Nature* **549**, 242 (2017).
  - [9] E. Farhi, J. Goldstone, and S. Gutmann, arXiv:1411.4028 (2014).
  - [10] E. Farhi and A. W. Harrow, arXiv preprint arXiv:1602.07674 (2016).
  - [11] J. R. McClean, M. E. Kimchi-Schwartz, J. Carter, and W. A. De Jong, *Physical Review A* **95**, 042308 (2017).
  - [12] O. Kyriienko, *npj Quantum Information* **6**, 1 (2020).
  - [13] R. M. Parrish and P. L. McMahon, arXiv preprint arXiv:1909.08925 (2019).
  - [14] T. A. Bespalova and O. Kyriienko, arXiv preprint arXiv:2009.03351 (2020).
  - [15] W. J. Huggins, J. Lee, U. Baek, B. O’Gorman, and K. B. Whaley, *New Journal of Physics* (2020).
  - [16] T. Takeshita, N. C. Rubin, Z. Jiang, E. Lee, R. Babbush, and J. R. McClean, *Physical Review X* **10**, 011004 (2020).
  - [17] N. H. Stair, R. Huang, and F. A. Evangelista, *Journal of Chemical Theory and Computation* **16**, 2236 (2020).
  - [18] M. Motta, C. Sun, A. T. Tan, M. J. O’Rourke, E. Ye, A. J. Minnich, F. G. Brandão, and G. K.-L. Chan, *Nature Physics* **16**, 205 (2020).
  - [19] K. Seki and S. Yunoki, arXiv:2008.03661 (2020).
  - [20] K. Bharti, arXiv preprint arXiv:2009.11001 (2020).
  - [21] K. Bharti and T. Haug, arXiv:2010.05638 (2020).
  - [22] A. Cervera-Lierta, J. S. Kottmann, and A. Aspuru-Guzik, *PRX Quantum* **2**, 020329 (2021).
  - [23] Y. Li and S. C. Benjamin, *Physical Review X* **7**, 021050 (2017).
  - [24] X. Yuan, S. Endo, Q. Zhao, Y. Li, and S. C. Benjamin, *Quantum* **3**, 191 (2019).
  - [25] M. Benedetti, M. Fiorentini, and M. Lubasch, arXiv preprint arXiv:2009.12361 (2020).
  - [26] K. Bharti and T. Haug, arXiv:2011.06911 (2020).
  - [27] S. Barison, F. Vicentini, and G. Carleo, arXiv:2101.04579 (2021).
  - [28] B. Commeau, M. Cerezo, Z. Holmes, L. Cincio, P. J. Coles, and A. Sornborger, “Variational hamiltonian diagonalization for dynamical quantum simulation,” (2020), arXiv:2009.02559 [quant-ph].
  - [29] K. Heya, K. M. Nakanishi, K. Mitarai, and K. Fujii, arXiv preprint arXiv:1904.08566 (2019).
  - [30] C. Cirstoiu, Z. Holmes, J. Iosue, L. Cincio, P. J. Coles, and A. Sornborger, *npj Quantum Information* **6**, 1 (2020).
  - [31] J. Gibbs, K. Gili, Z. Holmes, B. Commeau, A. Arrasmith, L. Cincio, P. J. Coles, and A. Sornborger, arXiv preprint arXiv:2102.04313 (2021).
  - [32] J. W. Z. Lau, K. Bharti, T. Haug, and L. C. Kwek, arXiv preprint arXiv:2101.07677 (2021).
  - [33] T. Haug and K. Bharti, arXiv preprint arXiv:2011.14737 (2020).
  - [34] M. Otten, C. L. Cortes, and S. K. Gray, arXiv preprint arXiv:1910.06284 (2019).
  - [35] K. H. Lim, T. Haug, L. C. Kwek, and K. Bharti, arXiv preprint arXiv:2104.01931 (2021).
  - [36] J. W. Z. Lau, T. Haug, L. C. Kwek, and K. Bharti, arXiv preprint arXiv:2103.05500 (2021).
  - [37] J. J. Meyer, J. Borregaard, and J. Eisert, arXiv preprint arXiv:2006.06303 (2020).
  - [38] J. J. Meyer, arXiv preprint arXiv:2103.15191 (2021).
  - [39] M. Schuld and N. Killoran, *Phys. Rev. Lett.* **122**, 040504 (2019).
  - [40] V. Havlíček, A. D. Córcoles, K. Temme, A. W. Harrow, A. Kandala, J. M. Chow, and J. M. Gambetta, *Nature* **567**, 209 (2019).
  - [41] T. Kusumoto, K. Mitarai, K. Fujii, M. Kitagawa, and M. Negoro, arXiv:1911.12021 (2019).
  - [42] E. Farhi and H. Neven, arXiv:1802.06002 (2018).
  - [43] K. Mitarai, M. Negoro, M. Kitagawa, and K. Fujii, *Physical Review A* **98**, 032309 (2018).
  - [44] J. R. McClean, S. Boixo, V. N. Smelyanskiy, R. Babbush, and H. Neven, *Nature communications* **9**, 4812 (2018).
  - [45] K. Sharma, M. Cerezo, L. Cincio, and P. J. Coles, arXiv preprint arXiv:2005.12458 (2020).
  - [46] M. Cerezo, A. Sone, T. Volkoff, L. Cincio, and P. J.

- Coles, arXiv preprint arXiv:2001.00550 (2020).
- [47] S. Wang, E. Fontana, M. Cerezo, K. Sharma, A. Sone, L. Cincio, and P. J. Coles, arXiv preprint arXiv:2007.14384 (2020).
- [48] L. Bittel and M. Kliesch, arXiv:2101.07267 (2021).
- [49] H.-Y. Huang, K. Bharti, and P. Rebentrost, arXiv preprint arXiv:1909.07344 (2019).
- [50] T. Haug, K. Bharti, and M. Kim, arXiv:2102.01659 (2021).
- [51] T. Haug and M. Kim, arXiv:2104.14543 (2021).
- [52] M. Larocca, P. Czarnik, K. Sharma, G. Muraleedharan, P. J. Coles, and M. Cerezo, arXiv preprint arXiv:2105.14377 (2021).
- [53] L. Vandenberghe and S. Boyd, SIAM review **38**, 49 (1996).
- [54] H. Wolkowicz, R. Saigal, and L. Vandenberghe, *Handbook of semidefinite programming: theory, algorithms, and applications*, Vol. 27 (Springer Science & Business Media, 2012).
- [55] P. Skrzypczyk, I. Šupić, and D. Cavalcanti, Physical review letters **122**, 130403 (2019).
- [56] J. Bae and L.-C. Kwek, Journal of Physics A: Mathematical and Theoretical **48**, 083001 (2015).
- [57] M. Ray, N. G. Boddu, K. Bharti, L.-C. Kwek, and A. Cabello, New Journal of Physics **23**, 033006 (2021).
- [58] K. Bharti, M. Ray, A. Varvitsiotis, A. Cabello, and L.-C. Kwek, arXiv preprint arXiv:1911.09448 (2019).
- [59] K. Bharti, M. Ray, A. Varvitsiotis, N. A. Warsi, A. Cabello, and L.-C. Kwek, Physical review letters **122**, 250403 (2019).
- [60] K. Bharti, M. Ray, Z.-P. Xu, M. Hayashi, L.-C. Kwek, and A. Cabello, arXiv preprint arXiv:2104.13035 (2021).
- [61] F. G. Brandão, A. Kalev, T. Li, C. Y.-Y. Lin, K. M. Svore, and X. Wu, arXiv preprint arXiv:1710.02581 (2017).
- [62] J. Van Apeldoorn, A. Gilyén, S. Gribling, and R. de Wolf, in *2017 IEEE 58th Annual Symposium on Foundations of Computer Science (FOCS)* (IEEE, 2017) pp. 403–414.
- [63] J. van Apeldoorn and A. Gilyén, arXiv preprint arXiv:1804.05058 (2018).
- [64] I. Kerenidis and A. Prakash, ACM Transactions on Quantum Computing **1**, 1 (2020).
- [65] F. G. Brandao and K. M. Svore, in *2017 IEEE 58th Annual Symposium on Foundations of Computer Science (FOCS)* (IEEE, 2017) pp. 415–426.
- [66] K. Mitarai and K. Fujii, Physical Review Research **1**, 013006 (2019).
- [67] E. Marianna, M. Laurent, A. Varvitsiotis, *et al.*, in *Discrete Geometry and Optimization* (Springer, 2013) pp. 105–120.
- [68] S. Boyd, L. El Ghaoui, E. Feron, and V. Balakrishnan, *Linear matrix inequalities in system and control theory* (SIAM, 1994).
- [69] M. F. Anjos and J. B. Lasserre, *Handbook on semidefinite, conic and polynomial optimization*, Vol. 166 (Springer Science & Business Media, 2011).
- [70] L. Lovász, IEEE Transactions on Information theory **25**, 1 (1979).
- [71] C. Budroni, A. Cabello, O. Gühne, M. Kleinmann, and J.-Å. Larsson, arXiv preprint arXiv:2102.13036 (2021).
- [72] A. Cabello, S. Severini, and A. Winter, Physical review letters **112**, 040401 (2014).
- [73] K. Bharti, T. Haug, V. Vedral, and L.-C. Kwek, AVS Quantum Science **2**, 034101 (2020).
- [74] M. Howard, J. Wallman, V. Veitch, and J. Emerson, Nature **510**, 351 (2014).
- [75] J. S. Bell, *Physics (Long Island City, N.Y.)* **1**, 195 (1964).
- [76] J. F. Clauser, M. A. Horne, A. Shimony, and R. A. Holt, *Phys. Rev. Lett.* **23**, 880 (1969).
- [77] N. Brunner, D. Cavalcanti, S. Pironio, V. Scarani, and S. Wehner, Reviews of Modern Physics **86**, 419 (2014).
- [78] V. Scarani, *Bell nonlocality* (Oxford University Press, 2019).
- [79] T. Haug and K. Bharti, “Nisq sdp solver,” <https://github.com/txhaug/nisq-sdp>.

## Appendix A: Hardware Efficient Circuit

In Fig. 6, we show the randomized quantum circuit that we use as one of our ansatz states for our demonstration examples for the NSS.

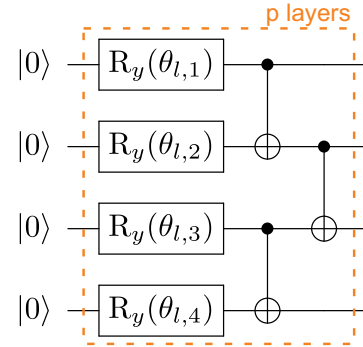


FIG. 6. Circuit of  $N$  qubits to generate ansatz state  $|\psi\rangle$ . It consists of  $p$  layers of  $N$  single qubit rotations around the  $y$  axis with randomized parameters  $\theta_{l,i}$ , followed by CNOT gates arranged in a nearest-neighbor chain topology.

## Appendix B: Proof for Positive Semidefinite Hybrid Density Matrix

Here, we show that the hybrid density matrix  $X_\beta$  is positive semidefinite when the coefficient matrix  $\beta$  is positive semidefinite.

*Claim 1.*  $X_\beta \succcurlyeq 0$  if and only if  $\beta \succcurlyeq 0$ .

*Proof.* We have

$$X_\beta \succcurlyeq 0 \iff \sum \beta_{i,j} \langle x|\psi_i\rangle \langle \psi_j|x\rangle \geq 0 \quad \forall \quad |x\rangle \in \mathcal{H}.$$

For a vector  $c^x$  of size  $M$ , defined via  $c_i^x \equiv \langle x|\psi_i\rangle$ , we have

$$X_\beta \succcurlyeq 0 \iff (c^x)^\dagger \beta c^x \geq 0 \quad \forall \quad |x\rangle \in \mathcal{H}.$$

Thus,

$$X_\beta \succcurlyeq 0 \iff \beta \succcurlyeq 0.$$

□



### Appendix C: Rank Constrained SDPs

We now study rank constrained SDPs. Note that solving rank-constrained SDPs is NP-hard. The famous max cut problem with  $n \times n$  weight matrix  $W$  admits the following rank one constrained SDP.

$$\begin{aligned} \max \quad & \frac{1}{2} \text{Tr}(WX) \\ \text{s.t.} \quad & X_{i,i} = 1 \quad \forall i \in [n], \\ & X \succcurlyeq 0, \\ & \text{rank}(X) \leq 1. \end{aligned} \quad (\text{C1})$$

#### 1. The Rank 1 Case

We have the following ansatz.

$$x_\alpha = \sum_i \alpha_i |\psi_i\rangle$$

$$X_\alpha = x_\alpha^\dagger x_\alpha$$

$$X_\alpha = \sum_{i,j} \alpha_i^\dagger \alpha_j |\psi_i\rangle \langle \psi_j|$$

By construction,

$$X_\alpha \succcurlyeq 0$$

This corresponds to the positive semidefinite cone constraint and holds for all values of  $\alpha$ . Also notice that

$$X_\alpha^\dagger = X_\alpha$$

by construction and thus  $X_\alpha$  is Hermitian. Let us assume that

$$C = \sum_k \beta_k U_k$$

and

$$A_i = \sum_l f_{i,l} U_l^{(i)}.$$

$\text{Tr}(CX_\alpha)$  translates to

$$\alpha^\dagger \mathcal{D} \alpha,$$

where

$$\mathcal{D}_{a,b} = \sum_k s_k \langle \psi_b | U_k | \psi_a \rangle.$$

The constraints  $\text{Tr}(A_i X_\alpha) = b_i$  translate to

$$\alpha^\dagger \mathcal{E}^{(i)} \alpha = b_i$$

where

$$\mathcal{E}_{a,b}^{(i)} = \sum_l f_{i,l} \langle \psi_b | U_l^{(i)} | \psi_a \rangle.$$

Thus, in the ansatz space, the standard form rank-constrained SDP reduces to

$$\min \alpha^\dagger \mathcal{D} \alpha \quad (\text{C2})$$

$$\text{s.t. } \alpha^\dagger \mathcal{E}^{(i)} \alpha = b_i$$

$\forall i \in [m]$ . This is a quadratically constrained quadratic program (QCQP). The quantum assisted eigensolver and iterative quantum assisted eigensolver [20, 21] can be framed as QCQP of the form of program C2.

#### 2. The Rank k Case

We have the following ansatz.

$$x_\alpha^p = \sum_i \alpha_i^p |\psi_i\rangle$$

$$X_{\alpha,\gamma} = \sum_{p=1}^k \gamma^p x_\alpha^{p\dagger} x_\alpha^p$$

$$X_{\alpha,\gamma} = \sum_{i,j,p} \gamma^p \alpha_j^{p\dagger} \alpha_i^p |\psi_i^p\rangle \langle \psi_j^p|$$

By construction,

$$X_{\alpha,\gamma} \succcurlyeq 0$$

for  $\gamma^p \geq 0 \quad \forall p \in [k]$ . This corresponds to the positive semidefinite cone constraint and holds for all values of  $\alpha^p$ . Also notice that

$$X_{\alpha,\gamma}^\dagger = X_{\alpha,\gamma}$$

by construction and thus  $X_{\alpha,\gamma}$  is Hermitian. Let us assume that

$$C = \sum_k s_k U_k$$

and

$$A_i = \sum_l f_{i,l} U_l^{(i)}.$$

$\text{Tr}(CX_{\alpha,\gamma})$  translates to

$$\sum_{p=1}^k \gamma^p \alpha^{p\dagger} \mathcal{D} \alpha^p,$$

where

$$\mathcal{D}_{a,b}^p = \sum_k s_k \langle \psi_b^p | U_k | \psi_a^p \rangle.$$

The constraints  $Tr(A_i X_{\alpha,\gamma}) = b_i$  translate to

$$\sum_{p=1}^k \gamma^p \alpha^{p\dagger} \mathcal{E}^{p(i)} \alpha^p = b_i$$

where

$$\mathcal{E}_{a,b}^{p(i)} = \sum_l f_{i,l} \langle \psi_b^p | U_l^{(i)} | \psi_a^p \rangle.$$

Thus, in the ansatz space, the standard form rank-constrained SDP for general  $k$  reduces to

$$\begin{aligned} \min \quad & \sum_{p=1}^k \gamma^p (\alpha^{p\dagger} \mathcal{D}^p \alpha^p) \\ \text{s.t.} \quad & \sum_{p=1}^k \gamma^p (\alpha^{p\dagger} \mathcal{E}^{p(i)} \alpha^p) = b_i \quad \forall i \in [m] \\ & \gamma^p \geq 0 \quad \forall p \in [k]. \end{aligned} \quad (\text{C3})$$

#### Appendix D: XOR Games SDP Formulation

**Definition 2.** Two prover game: Given a predicate  $V : \mathcal{X} \times \mathcal{Y} \times \mathcal{A} \times \mathcal{B} \rightarrow \{0, 1\}$  and a probability distribution  $\pi$  on  $\mathcal{X} \times \mathcal{Y}$ , a two prover game  $\mathcal{G} = (\mathcal{X}, \mathcal{Y}, \mathcal{A}, \mathcal{B}, V, \pi)$  involves two provers and one verifier, which proceeds as follows:

1. The verifier samples a pair of questions  $(x, y) \in \mathcal{X} \times \mathcal{Y}$  according to the probability distribution  $\pi$ .
2. The verifier sends  $x$  and  $y$  to the two provers and receives answers  $a \in \mathcal{A}$  and  $b \in \mathcal{B}$  respectively.
3. The verifier applies the predicate  $V : \mathcal{X} \times \mathcal{Y} \times \mathcal{A} \times \mathcal{B} \rightarrow \{0, 1\}$  and accepts the answers if the outcome is 1, rejects otherwise.

The size of the sets  $\mathcal{A}$  and  $\mathcal{B}$ , say some integer value  $k$  is assumed to be equal and is referred to as *alphabet size* of the two prover game.

**Definition 3.** Unique two prover game: A two prover game  $\mathcal{G} = (\mathcal{X}, \mathcal{Y}, \mathcal{A}, \mathcal{B}, V, \pi)$  where the predicate  $V : \mathcal{X} \times \mathcal{Y} \times \mathcal{A} \times \mathcal{B} \rightarrow \{0, 1\}$  returns value 1 iff  $b = \pi_{x,y}(a)$ , 0 otherwise for  $(x, y) \in \mathcal{X} \times \mathcal{Y}$  and outputs  $a, b \in \mathcal{A} \times \mathcal{B}$ . Here  $\pi_{x,y}$  is a permutation of  $[k]$ .

**Definition 4.** XOR game: A unique two prover game with alphabet size 2 is known as XOR game. XOR games

are restricted form of two prover nonlocal game where  $\mathcal{A} = \mathcal{B} = \{0, 1\}$  and the predicate  $V$  takes the form

$$V(a, b, x, y) = \begin{cases} 1 & \text{if } a \oplus b = f(x, y) \\ 0 & \text{if } a \oplus b \neq f(x, y) \end{cases} \quad (\text{D1})$$

for some given function  $f : \mathcal{X} \times \mathcal{Y} \rightarrow \{0, 1\}$ . The function  $f$  determines whether the two parties should agree or disagree for each question pair  $(x, y)$ .

The maximum probability of success that the two provers can achieve is known as value of the game and often denoted by  $\text{val}(\mathcal{G})$ . For a given XOR game  $\mathcal{G}$  and any strategy, the bias of that strategy is the probability it wins minus probability it loses. The bias of a XOR game  $\mathcal{G}$  is the supremum bias over all possible strategies. Let us denote the supremum bias as  $\epsilon(\mathcal{G})$ . It is easy to see that

$$\text{val}(\mathcal{G}) = 0.5 + 0.5 * \epsilon(\mathcal{G}) \quad (\text{D2})$$

For every XOR game  $\mathcal{G}$ , we further define a matrix  $D$  as

$$D(x, y) = \pi(x, y) (-1)^{f(x, y)}, \quad (\text{D3})$$

where  $f$  determines the value of the predicate  $V$  according to D1. Using  $D$ , one can further define a symmetric matrix  $H$  as

$$H = \frac{1}{2} \begin{pmatrix} 0 & D \\ D^T & 0 \end{pmatrix}. \quad (\text{D4})$$

The bias of an XOR game is formulated via  $H$  as the following SDP.

$$\begin{aligned} \max \quad & \text{trace}(HZ), \\ \text{s.t.} \quad & Z_{i,i} = 1 \quad \forall i \in [h], \\ & Z \succcurlyeq 0, \\ & Z \in \mathcal{S}_+^n. \end{aligned} \quad (\text{D5})$$

Here,  $h$  denotes the size of the  $H$  matrix. For the CHSH game, we have  $f_{\text{CHSH}}(x, y) = x \wedge y$  where  $\wedge$  is the logical AND operator. Thus, the  $D$  matrix for the CHSH game is given by

$$D_{\text{CHSH}} = \begin{pmatrix} 0.25 & 0.25 \\ 0.25 & -0.25 \end{pmatrix}.$$